An injectable scaffold based on crosslinked hyaluronic acid gel for tissue regeneration

Yang, Rue; Tan, Linhua ; Cen, Lian ; Zhang, Zhibing

DOI:
10.1039/c5ra27870h

An Injectable Scaffold Based on Crosslinked Hyaluronic Acid Gel for Tissue Regeneration

Rui Yang[1#], Linhua Tan[1#], Lian Cen[1]*, Zhibing Zhang[2]*

[1]Shanghai Key Laboratory of Multiphase Materials Chemical Engineering, Department of Product Engineering, School of Chemical Engineering, East China University of Science and Technology. No.130 Mei Long Road, Shanghai, 200237, China.

[2]School of Chemical Engineering, The University of Birmingham, Edgbaston, Birmingham, B15 2TT, UK.

[#]These authors contributed equally to this work.

Running title: Crosslinked Hyaluronic Acid Gel as An Injectable Scaffold

* To whom correspondence should be addressed.

Tel: +86-21-64252808; Fax: +86-21-64253159.

E-mail: Prof. Lian Cen: cenlian@hotmail.com

Prof. Zhibing Zhang: z.zhang@bham.ac.uk

Abstract

Injectable scaffolds have great potential in special applications of regenerative medicine. In this study, hyaluronic acid hydrogels (HAGs) were prepared by crosslinking hyaluronic acid (HA) with 1,4-butanediol diglycidyl ether (BDDE). Applications of HAG as an injectable scaffold for regenerating functional tissues were proposed by matching its viscoelastic properties with those of biological tissues. The effect of BDDE concentration on different properties of HAGs was explored. Swelling properties, cross-sectional morphology, and BDDE residues of the resulting gels were investigated. Rheological properties of different HAGs were measured by monitoring their storage modulus (G') and loss modulus (G") and compared with those of biological tissues. It was shown that HAGs (BDDE from 0.4 vol% to 1.0 vol%) possessed great water absorbing capability with swelling ratios ranging from 99.7 to 78.9. The higher the concentration of the crosslinker used, the more rigid the resulting hydrogel, subsequently the lower the swelling ratio would be and the higher the G' and G" values as well. Similar viscoelastic behaviors were found between HAGs and biological tissues, such as epidermis, dermis, articular cartilage and tooth germ. SEM revealed that HAG obtained at 0.4 vol% BDDE had pore diameters ranging from a few microns to around 100 μm with a high degree of interconnectivity. The feasibility of this HAG, as an injectable scaffold, to regenerate cartilage and dentin-pulp complex was then demonstrated using a preliminary subcutaneous microenvironment. The current study could be a reference to account how a crosslinked HA gel should be chosen for specific tissue regeneration.

Keywords: hyaluronic acid gel, regeneration, injectable scaffold, crosslinking, viscoelastic

1. Background

A scaffold-based tissue engineering strategy to repair or regenerate impaired/damaged tissues has been studied extensively in last decades, which benefits to the functional restoration of tissue structure and physiology.[1-9] An appropriate scaffold should be non-toxic, bioactive, physiologically compatible, and the three dimensional microenvironment it provides should be favorable for cell migration and cellular organization into a desired tissue structure.[10,11] In addition, how a scaffold is utilized would also influence the final outcome. Conventionally, preformed scaffolds with specific structures, after being combined with seeded cells/growth factors, were implanted into the defect sites via tedious surgical procedures.[12] Injectable scaffolds, one of the recent focuses, can be applied by administration directly at a desired location in a minimally invasive manner.[13,14] Obviously, the possible risk of infection during surgery could be minimized, while less scarring and/or pain would be accompanied.[15] Injectability also endows a scaffold the ability to easily fill irregularly shaped defects, thus improving contact with surrounding tissues.[14,16-18] Moreover, compared to pre-shaped scaffolds, seed cells and/or activity factors could be distributed more uniformly within injectable scaffolds before injection, simply and quickly by mixing.[19,20] The above merits make injectable scaffolds great potential in special applications of regenerative medicine.[21-25]

As to materials used to prepare injectable scaffolds, hyaluronic acid (HA) is one of favorites. As a linear polysaccharide that consists of alternating units of a repeating disaccharide (β-1,4-D-glucuronic acid-β-1,3-N-acetyl-D-glucosamine), HA, is found primarily in the (extracellular matrix) ECM and pericellular matrix, but has also been shown to occur intracellularly.[26] The biological properties, such as biocompatibility, biodegradability, bioactivity and non-immunogenicity of HA along with its unique viscoelastic nature endow HA the very ability to mediate its activity in cellular signaling, wound repair, morphogenesis, and matrix/morphologic organization.[26-29] In addition, the role of HA in some special tissues and its rich contents are of strong interests. For example, HA is a major component of synovial fluid and cartilage, and

is of great importance to maintain chondrocyte functions.[30,31] HA contributes to the initial development of dentin matrix and dental pulp, and is beneficial to wound healing.[32,33] HA and its derivatives have been clinically used as medical products, especially as skin fillers, for over three decades.[34]

Depolymerization of HA chains (polysaccharides) in situ would usually occur via enzymatic or free radical degradation quickly and thereafter yield smaller HA units (oligosaccharides) which soon enter the circulatory system and are eliminated by the liver/kidneys. Hence, to be used as an injectable scaffold, HA should be crosslinked to increase its longevity to match tissue growth via different crosslinking agents. One of crosslinkers, 1,4-butanediol diglycidyl ether (BDDE), was used in the majority of the market-leading HA fillers whose stability, biodegradability, and long safety record have spanned more than 15 years.[35] In our previous work, BDDE-crosslinked HA gels (HAGs) were successfully used as an injectable scaffold in the form of microparticles to in-situ regenerate dentin-pulp complex in porcine.[1]

However, there are important questions which remain to be answered, i.e. what can happen when such kind of scaffold, HAG, is implanted, how can the toxic residue of BDDE used for crosslinking be monitored, and how its mechanical properties can be manipulated so as to match the target tissue as an injectable scaffold? In this work, BDDE crosslinked HA gels were prepared and the effect of its concentration on different properties of HA gels was explored. Rheological properties of different HA gels were measured and compared with those of biological tissues. A simple and sensitive method was developed to monitor the residue of BDDE within gels. After assessing the cytotoxicity of HA gels, its general application as an injectable scaffold was demonstrated. It is believed that the current study would serve as a reference to account how a crosslinked HA gel should be chosen for specific tissue regeneration and how to understand its role which might be different to traditional views on scaffolds.

2. Methods

2.1 Materials

Hyaluronic acid sodium salt (HA, also called hyaluronan or sodium hyaluronate) with an average molecular weight of 1.5×10^6 Da, was supplied by Shangdong Freda Biopharm Co., Ltd. (Jinan, China) as dry powders. 1,4-butanediol diglycidyl ether (BDDE) was purchased from Sigma Chemical (St. Louis, MO, USA). Unless otherwise specified, all other chemical reagents used were supplied by Sinopharm Chemical Reagent, of analytical grade and used as received without further purification.

2.2 Preparation of HAG via crosslinking

HA was first dissolved in 1% NaOH at a concentration of 10 wt%, after which BDDE was added to the HA solution with vigorous stirring. The final concentrations of BDDE were 0.4 vol%, 0.6 vol%, 0.8 vol% and 1 vol%, respectively. The solution was then allowed to crosslink at 40 °C for 5 h, followed by being dried at room temperature for 3 days (Scheme 1). Phosphate buffered saline (PBS: NaCl, 9 mg/mL; KH_2PO_4, 0.03 mg/mL; $Na_2HPO_4 \times 2H_2O$, 0.14 mg/mL; pH=7) of 500 mL was then added to the above crosslinked HA or HAG to make it swell, after which HAG was put into dialysis bag and dialyzed sequentially with excessive deionized (DI) water and PBS to remove the residual BDDE. The resulting gel was adjusted with PBS to obtain HAG with a HA concentration of 20 mg/mL and then smashed with a homogenizer to obtain gel particles of 0-400 μm. Before being used, the obtained injectable HAG scaffold was sterilized in a high-pressure steam sterilizer set at 120 °C, 20 min.

2.3 Swelling behaviors of HAG

To examine the swelling behaviors, hydrogels prepared under different BDDE concentrations were soaked, respectively, in DI water at 37 °C until swelling equilibrium had been reached. The hydrogels were then taken out and weighed (BSA124S, Sartorius, Goettingen, Germany) after the removal of excess water on their surfaces with filter papers. The hydrogels were dried under vacuum at room

temperature for 3 days to achieve constant weight. The equilibrium swelling ratio (SR) was calculated based on the following equation:

$$\text{Swelling ratio}\,(\text{SR}) = \frac{W_S - W_0}{W_0}$$

Where Ws and W_0 are the weights of the swollen hydrogel and the corresponding dried hydrogel, respectively. All experiments were performed in triplicate and swelling ratios were given without units as mean ± standard error of mean.

2.4 Rheological analysis of porcine tissues and HAGs

The rheological properties were elucidated by dynamic oscillatory measurements using an Anton Paar-Physica MCR 301 Rheometer (Anton Paar GmbH, Germany) with a 25 mm diameter parallel plate geometry (PP25). The epidermis (face), dermis (face), and articular cartilage from adult porcine, tooth germ obtained from newly born pigs, and different HAGs (after sterilization) were carefully placed into the lower plate after which the upper plate was lowered to a 1 mm gap. After that, dynamical oscillatory frequency sweeps for porcine tissues and HAGs were performed at 37 °C (physiological temperature) with constant strain (1%) and the frequency was set from 0.1 to 10 Hz. The storage modulus (G') and loss modulus (G") as a function of frequency were recorded by the associated software.

2.5 Morphology of cross-sections of HAGs

Cross-sections of hydrogels obtained from different concentrations of BDDE were characterized by scanning electron microscopy (SEM). Briefly, after reaching swelling equilibrium, hydrogels were quickly frozen in liquid nitrogen and fractured quickly followed by being freeze-dried for 48 h. After being coated with an ultrathin layer of gold/Pt, the cross-sectional morphologies of the lyophilized gels were observed by a Nova Nano SEM (Tokyo, Japan).

2.6 Determination of BDDE residues within HAGs

A highly sensitive method based on fluorescent spectrophotometry was applied to determine the amount of BDDE.[36] This method makes use of strong fluorescent substance produced by BDDE and nicotinamide where excitation wavelength and emission wavelength were located at 370 nm and 430 nm, respectively. The

fluorescent intensity appeared, which can be detected using a fluorescent spectrophotometer, is proportional to the amount of BDDE.

Each freshly prepared HAG sample (prepared from 0.5 g HA crosslinked with different amounts of BDDE) in its swelling equilibrium was added with a soaking solution of 50 mL DI water. The samples were then shaken at a speed of 50 rpm using a shaking table (HY-5, Jiangsu, China) at room temperature and the DI water was renewed every 24 h. The soaking solution of 200 μL was mixed with a freshly prepared nicotinamide solution (100 μL, 125 mmol L^{-1}). The mixed solution was incubated in a water bath at 37 ^{o}C for 120 min. After that, acetophenone solution (1 mL, 15 vol% in ethanol) and potassium hydroxide solution (1 mL, 1 mol L^{-1}) were added into the above mixture. After being incubated in an ice bath for 10 min, formic acid (5 mL) was added into this mixture, which was then heated at 60 ^{o}C using a water bath for 5 min and subsequently cooled in an ice bath for 10 min. The resulting solution after being kept at room temperature for 15 min was finally subjected to fluorescent intensity recording using a fluorescent spectrophotometer (Cary Eclipse, USA) with an excitation wavelength at 370 nm and an emission wavelength at 430 nm. A standard curve using serial dilutions of BDDE was first established to determine the relationship between the fluorescent intensity and BDDE concentration. As determined, the method has an excellent linear range of 0.5-8.0 μg mL^{-1} BDDE. Below the low threshold, the intensity was undetectable with high background interference. The determined BDDE concentration of the soak solution was termed as the released amount based on the soaking times as shown in Table 1. Each measurement was performed in triplicate and the average values were reported.

2.7 Cytotoxicity of HAG on human fibroblasts

This study was approved by the ethic committee of Shanghai Ninth People's Hospital Affiliated School of Medicine of Shanghai Jiao Tong University and informed consent from all of the patients was obtained. Fresh human foreskin specimens were obtained from donors (aged from 5 to 12 years) who received a routine circumcision procedure at Shanghai Children’s Hospital, China. The specimens were washed with sterile phosphate-buffered saline (PBS), and cut into

small pieces (1-2 mm^3) which were then digested with 0.1% dispase (Worthington, Lakewood, NJ) at 4 °C overnight. The epidermal layers were removed, and the remaining dermal parts were further digested with 0.1% collagenase (Worthington, Lakewood, NJ) in Dulbecco's Modified Eagle Medium (DMEM, Invitrogen, USA) for 3 h by gentle agitation at 37 °C. The digested cells were then forced to pass through a 100 μm cell strainer (BD Biosciences, USA) and further centrifuged (Allegra 64R Centrifuge, Beckman Coulter, California, USA) at 1500 rpm for 5 min. The cells were collected by resuspension in low-glucose DMEM supplemented with 10% fetal bovine serum (FBS, Hyclone, USA), L-glutamine (300 mg/mL), vitamin C (50 mg/mL), penicillin (100 U/mL), and streptomycin (100 mg/mL) (all from Sigma-Aldrich, USA). After the cell suspension was plated for 24 h, the plates were washed thoroughly with PBS to remove residual non-adherent cells. When 90% confluence was reached, cells were detached and subcultured at 1×10^4 cells/cm^2 in the culture plates. For the following experiment, cells of passage 3-5 were used.

The in vitro cytotoxicity tests of HAG obtained from 0.4% BDDE concentration was determined by 3-(4,5-dimcthylthioazol-2-yl)-2,5-diphenyl-tetrazolium bromide (MTT) assay. The above cells in their logarithmic growth were seeded at a density of 5000 cells per well in 96-well plates with 100 μL of culture medium. After 24 h of incubation, the medium was removed. The cells were incubated with 100 μL of the above culture medium (negative control), or 100 μL medium containing either 0.5 mg/mL or 1 mg/mL cross-linked HA gels, or 100 μL medium containing 64 mg/mL phenol (positive control), respectively. Cells were incubated with these treatments for 2 d, 4 d or 7 d, respectively, and the respective viability of cells was then determined by MTT assay. Briefly, 20 μL of MTT (5 mg/mL in Ca^{2+} and Mg^{2+} free PBS, Sigma, St. Louis, MO, USA) was added to each well at the time of incubation and the cells were incubated for another 4 h at 37 ^oC for MTT formazan formation. The medium was then removed carefully and 200 μL dimethyl sulfoxide (DMSO, Sigma) was added to each well to dissolve the formazan crystals. The plates were shaken for 10 min and then the absorbance at a wavelength of 490 nm of each well was read on in a spectrophotometric DIA reader (Elx 800G, DIALAB GMBH, Vienna, Austria). Data

were presented as mean ± standard error from three individuals, and each of them was the mean of triplicate experiments.

2.8 Microscopic observation of HAG injectable scaffold and its subcutaneous degradation in nude mice

In order to have a gross morphology observation, the injectable HAG scaffold was added with a few drops of black ink, followed by being observed under a florescent microscope (DYF-330C, Shanghai, China). The above injectable HAG scaffold (0.2 mL) was injected subcutaneously into the dorsum of ~5 weeks old male nude mice either for 15 or 36 weeks to evaluate its degradation condition with time.

2.9 Regeneration of cartilage-like tissue subcutaneously in nude mice using injectable HAG scaffold

The surgical procedures were permitted by the Animal Care and Experimental Committee of School of Medicine, Shanghai Jiao Tong University. Cartilage tissue was harvested in sterile conditions from the articular cartilage of the pigs that were euthanized with an overdose of pentobarbital (100 mg kg^{-1} IV) according to the method reported previously.[37-39] The articular cartilage was cut into 2 × 2 × 1 mm^3 slices and washed twice with PBS. After being digested with 0.25% trypsin plus 0.02% EDTA (HyClone, USA) at 37 °C for 30 min, the cartilage slices were further digested at 37 °C with 0.1% (w/v) collagenase II for 12-16 h. The resulting chondrocytes were harvested, counted, and seeded onto culture dishes at a cell density of 2.5 × 10^4 cells cm^{-2} for culture and subculture in DMEM with 10% fetal bovine serum (FBS) (Hyclone, USA). The chondrocytes were expanded to Passage 1 for further experiments. The above cultured first passage chondrocytes were mixed with HAG scaffold (pre-incubated at 37 ^oC for 3 h) at a ratio of 2×10^7 cells/mL scaffold. The resulting cell-scaffold composites were immediately injected subcutaneously into the dorsum of ~5 weeks old male nude mice.

2.10 Regeneration of dentin-pulp complex subcutaneously in nude mice using injectable HAG scaffold

Tooth buds were isolated from jaws of newly born porcine and washed with 0.25% chloramphenicol solution for 3 times. The tooth bud tissue was then minced

into pieces (< 2 mm^3) , and enzymatically treated with 0.15% collagenase (NB4 Standard Grade, SERVA) and 0.5 U/mL dispase II (Neutral protease, Roche) in DMEM/F12 (1:1) (HyClone) with 15% fetal bovine serum (FBS) (HyClone) for 1.5 h at 37 °C. After that, the digested tooth bud tissues were strained with nylon filter (100-μm pores) and the harvested primary individual dental bud cells were cultured with DMEM/F12 (1:1) with 15% FBS and antibiotic/antimycotic solution (300/mL penicillin G, 300 μg/mL streptomycin, 0.75 μg/mL amphotericin B) (HyClone) at an incubator at 37 °C with 5% CO_2.[40] These cells were cultured for 5~7 days before reaching confluence and they formed a mixed population of epithelial- and fibroblast-like cells. The cells were then digested with 0.25% trypsin for 1~2 min, whereby dental mesenchymal cells (DMCs) were digested and most of epithelial cells were still adherent to the plastic surface of the cell culture dish. The digested cells were further cultured in the above medium without any antibiotic/antimycotics. Due to the difference in the sensitivity to trypsin and medium requirement, the residual epithelial cells gradually lost from the culture, leaving only the mesenchymal cells.[41] DMCs of passage 3 were used for further experiments.

The above cultured third passage DMCs were mixed with HAG scaffold (pre-incubated at 37 ^oC for 3 h) at a ratio of 5×10^7 cells/mL scaffold, further supplemented with BMP-4 of different concentrations (25 μg/mL, 12.5 μg/mL and 6.25 μg/mL respectively). The resulting cell-scaffold composites were immediately injected subcutaneously into the dorsum of ~5 weeks old male nude mice.

2.11 Histology and immunohistochemical analysis

When the samples were harvested, the animals were treated with euthanasia. The samples were then removed and washed with PBS, followed by being fixed in 4% paraformaldehyde at 4 ^oC for 24 h, demineralized with 10% EDTA at room temperature for several months (mineralized tissue). Samples were processed for paraffin sectioning, and the sections (5 μm-thick) were performed hematoxylin-eosin (H&E), Masson (MAIXIN.BIO) and immunohistochemical staining. The primary antibody used for the immunohistochemical analysis was rabbit anti-human dentin sialoprotein (DSP) polyclonal antibody (H-300) (1:100 dilution) (Santa Cruz). The

second antibody used was Envision+ system-HRP labeled polymer anti-rabbit (Dako), and liquid DAB+ substrate chromogen system (Dako) was used as well.

3 Results and discussion

3.1 Swelling behaviors of HAG

To reveal the effect of BDDE concentration on the swelling properties of hydrogels, HAGs after crosslinking were immersed in DI water to reach their corresponding equilibria which were monitored by mass at room temperature. As displayed in Fig. 1, all HAGs possessed great water absorbing capability. At the lowest BDDE concentration used (0.4 vol%), the HAG had a swelling ratio of around 100. With the increase in BDDE concentration, swelling ratio of the resulting HAGs decreased correspondingly. When the highest BDDE concentration was used (1.0 vol%), the swelling ratio of respective HAG was decreased to 78.9. Significant difference was observed in the swelling ratios of HAGs obtained from 0.4 vol% and 0.6 vol% ($p < 0.05$, Fig. 1). This was also the case for samples obtained from 0.6 vol% and 0.8 vol% ($p < 0.05$, Fig. 1), whereas no significant difference was observed in the swelling ratio between samples obtained from 0.8 vol% and 1.0 vol% ($p > 0.05$, Fig. 1). It could be expected that the higher the concentration of BDDE used, the more the rigidity of the resulting hydrogel, as more crosslinking points would be yielded. The higher the rigidity of the hydrogel, the lower the swelling ratio was. But it would be possible that at BDDE concentrations higher than 0.8 vol%, this trend was compromised by the BDDE crosslinking efficiency. Obviously, BDDE concentration in the above range is one of key factors in controlling swelling ratio of HAG.

3.2 Rheological properties of porcine tissues and HAGs

The rheological properties of HAGs were characterized by monitoring the storage modulus (G') and loss modulus (G") as a function of frequency through rheometry, which revealed the effect of BDDE concentration used for crosslinking on the viscoelasticity of HAGs (Fig. 2a and b). G' and G" of different HAGs exhibited similar nonlinear rheological behaviors whose values increased with the increase in frequencies, implying the existence of a similar microstructure. It was noted clearly that for each HAG, G' was far higher than G" in the range of whole frequencies, which means the majority of the energy was stored in the deformation of hydrogel

itself. The highly elastic nature of these hydrogels was thus indicated. It was also displayed in Fig. 2a and b that both G' and G" values increase with the increasing BDDE concentration from 0.4 vol% to 1.0 vol% within the tested frequency range.

It was revealed that the local matrix stiffness on cells has important implications for their development, differentiation, disease and regeneration.[42] At the macro scale, elasticity is evident in a solid tissue that can recover its shape within seconds after mild poking and pinching, or even after sustained compression. At the cellular scale, normal tissue cells probe elasticity as they anchor and pull on their surroundings. A normal tissue cell not only applies forces, but also responds through cytoskeleton organization to the resistance that the cell senses, regardless of whether the resistance derives from normal tissue matrix, synthetic substrate, or even an adjacent cell.[42,43] It was thus suggested that mechanical properties of the substrate or scaffold can profoundly affect cell locomotion, growth, and differentiation, and scaffolds with similar elasticity to target tissue would be preferable for regeneration.[42-44] Therefore, the viscoelastic properties of HAGs were thus compared with some tissues, such as epidermis, dermis, articular cartilage and tooth germ, in order to verify their feasibility as injectable scaffolds for tissue regeneration. As displayed in Fig. 3a and b, dynamic oscillatory frequency sweep curves (G' and G") for epidermis, dermis, articular cartilage and tooth germ exhibited similar nonlinear rheological behaviors to those of HA hydrogels (Fig. 2a and b), indicating the similar viscoelastic properties. By simply varying the BDDE concentration, it would be possible to obtain HA hydrogels that possess close viscoelastic properties to those of specific tissues.

HA has been approved by the Food and Drug Administration (FDA) simply as a dermal filler. In 2006, cosmetic injections of HA were known to be the second most popular non-surgical procedure for women and the third most popular procedure for men.[45-48] To overcome its short half-life, HA is chemically crosslinked to extend duration as a dermal filler via different crosslinkers or different procedures.[49] As a dermal filler, HA or HAG is not involved in the structure of collagen and does not enhance the shortage of HA in aged skin, but simply works by augmenting volume.[45,50] In the current work, it's the role of HAG as a filler, especially as a

cell-delivery filler to augment volume could stand based on its similar viscoelastic properties to both epidermis or dermis.

Among the natural polymers, HA was proven to be of fundamental priority for cartilage homeostasis and chondrocyte microenvironment. Therefore, series of HA derivatives have long been investigated as scaffolds or delivery matrixes for cartilage repair. For example, PEGDA crosslinked thiolated HA and gelatin were used for cell therapy to deliver mesenchymal stem cells to full-thickness defects in the patellar groove of rabbit femoral articular cartilage.[51] Elisseeff et al. pioneered the use of a photopolymerization process for the encapsulation of chondrocytes in HA based hydrogel networks for treating damaged cartilage tissue.[52-54] However, these HA hydrogels were clinically impractical because of the complexity of the chemistry and toxicity of preparation. Most of those HA based developments were just served as preclinical usages, as from a regulatory point of view, the involved chemistry might be problematic for development of a clinical product for cell delivery, even though their biological activities were preserved.[55] Regarding our current developed HAG, firstly the BDDE was already used in the majority of the market-leading HA fillers whose stability, biodegradability, and long safety record have spanned more than 15 years. Secondly, the BDDE residue could be carefully monitored. Thirdly, the crosslinking process was relatively simple and could be easily scaled up.

3.3 Morphology of cross-sections of HAGs

The morphological structure of HAGs was demonstrated by observing the cross-sections of lyophilized samples via SEM as shown in Fig. 4. It was found that all HAGs had a quite homogeneous porous structure. As to the HAG obtained from 0.4 vol%, the pores were well interconnected and formed an interconnected honeycomb structure (Fig. 4 A1 and A2). The degree of interconnectivity decreased with the increase in BDDE concentration used for obtaining HAGs (Fig. 4 A1-D1, A2-D2). Moreover, at the highest BDDE concentration, the porous structure was quite compact with the lowest degree of interconnectivity (Fig. 4 D1 and D2). It seems that the mean pore size of the porous network decreased with the increase in BDDE concentration. For instance, samples obtained from 0.4 vol% BDDE exhibited a mean

pore size of around 100 μm (Fig. 4 A2), which was gradually reduced to approximately 50 μm when BDDE concentration was increased to 1.0 vol% (Fig. 4 D2). Most probably, it was due to the fact that more crosslinking points were achieved within the HA macromolecular chains at a higher BDDE concentration. Since interconnectivity was very important for cellular communication and cell growth,[56,57] HAG obtained at 0.4 vol% BDDE with a mean pore size of 100 μm was selected for the following in vitro and in vivo evaluation as an injectable scaffold.

3.4 BDDE residues within HAG

Since BDDE itself was toxic, it is necessary to monitor its residue amount within the HAGs. As shown in Table 1, for all samples, the first released amounts of BDDE were higher than their respective following release. The reason for this might be that a thimbleful of residual BDDE could easily escape from the highly porous network structure when immersed in DI water. Reasonably, the released amount increased with the increase in BDDE concentration. Moreover, the fourth release of HA hydrogel (0.4 vol%) was already under the detection limit, suggesting that the residual BDDE of this sample had readily been removed. The relatively easy removal of toxic residues further ensured the suitability of this HAG as an injectable scaffold in the following applications.

3.5 Gross morphology and cytotoxicity of HAG on human fibroblasts

The particles size of prepared HAG was in the range of 0-400 μm (Fig. 5a and b). These gels in the form of irregular microparticles could be easily injected via a syringe (30G), facilitated by their elastic nature as determined by their rheological test.

The viabilities of cells incubated with the negative control (culture medium), 0.5 mg/mL, 1 mg/mL HAG (0.4 vol% BDDE) and the positive control (culture medium containing phenol) for 2 d, 4 d and 7 d are shown in Fig. 6. At the time point of 2 d, no significant difference in the absorbance can be observed between any two groups. With the increase in culture time to 4 d, the absorbance of negative control increased, whereas the one of positive control decreased significantly compared to their respective values at 2 d. The absorbance of either 0.5 mg/mL HAG group or 1 mg/mL

HAG group had a similar trend of increase from 2 d to 4 d to that of the negative control. There was a minor increase in absorbance of the 1 mg/mL HAG group was comparable with that of the negative control at 4 d ($P < 0.05$), but no difference in absorbance was observed between the 0.5 mg/mL HAG group and 1 mg/mL HAG group ($P > 0.05$). With the further increase in culture time to 7 d, the absorbance of negative control kept on increasing. This was also the case for 0.5 mg/mL and 1 mg/mL HAG groups, indicating that cells within these two groups were in a similar growth rate to those in culture medium. No significant difference was observed between negative control and 0.5 mg/mL group ($P > 0.05$), or negative control and 1 mg/mL group ($P > 0.05$). The one of positive control at 7 d was at a low absorbance which is close to the background level. Therefore, non-cytotoxicity nature of the injectable HAG scaffold could be confirmed.

3.6 Degradation of injectable HAG scaffold subcutaneously in nude mice

Gross views of pristine injectable HAG scaffold 15 and 36 weeks after being injected subcutaneously in nude mice are shown in Fig. 7 A and B, respectively. No tissue growth within the scaffold could be located except a thin layer of fibrous encapsulation both at 15 (Fig. 7 A1-A3) and 36 weeks (Fig. 7 B1-B3) according to their respective histological staining. At both time points, HAG (green arrow head) with a high content of water still occupied the whole samples, but most of the HAG fragments would be lost during H&E processing (Fig. 7 A1, A2, B1 and B2). Degradation with time could be indicated since the same amount of HAG had experienced shrinkage in its volume with time (Fig. 7 A and B). These results then were consistent with the statement mentioned above that as a dermal filler, HA or HAG is not involved in the structure of collagen and does not enhance the shortage of HA in aged skin, but simply works by augmenting volume.[45,50]

3.7 Regeneration of cartilage-like tissue subcutaneously in nude mice using injectable HAG scaffold

The in vivo construction condition before sample harvest is shown in Fig. 8 A. The harvested sample in shown in the inset here, suggesting that the initial fluent cell-scaffold complex already turned into a solid tissue for 12 weeks after being

constructed subcutaneously in nude mice. The further histological overall view and high magnification observation are shown in Fig. 8 B and C, respectively. Lacuna-like structure, typical cartilage characteristics, in the whole sample can easily be located. HAG fragments still remained within the sample.

3.8 Regeneration of dentin-pulp complex subcutaneously in nude mice

The in vivo construction process immediately after injection and before sample harvest of the constructs (DMCs+HAG+BMP-4) is shown in Fig. 9 A and B. From the gross views of the samples harvested, it can be observed that the initial cell/scaffold composites supplemented with different concentrations of BMP-4 were already mineralized at the time when they were harvested as shown in Fig. 9 C, D and E. Therefore, before they were further subjected to histological staining, demineralization was necessary for obtaining paraffin slices.

Overall views of H&E staining of the regenerated tissues are shown in Fig. 10 A, B and C, respectively (A: 25 μg/mL, B: 12.5 μg/mL, C: 6.25 μg/mL). All of the samples obtained from different concentrations of BMP-4 exhibited island-like features (Fig. 10 A-C). As to the sample obtained from the highest amount of BMP4, within localized areas of higher magnifications (Fig. 10 A1, A2 and A3), there were well organized dentinal tubules (white arrow head), columnar odontoblast-like cells (yellow arrow head) with polarized basal nuclei and blood vessels (black arrow head). Those cells (yellow arrow head) aligned against the regenerated dentin-like tissue, while those dentinal tubules (white arrow head) arranged radially from the pulp-like tissue. The above was typical dentin-pulp like features. When the BMP4 concentration was lowered to 12.5 μg/mL, the organization of those dentinal tubules was not as orderly as that of 25 μg/mL (Fig. 10 B1-B3). Moreover, the cell density within dentin-like area was higher than that in similar area of Fig. 10 A1-A3. However, with the further decrease in BMP4 concentration to 6.25 μg/mL, although the above dentin-pulp like feature could still be observed, bony-like tissue formation with hypertrophic cells was also located within the sample as shown in Fig. 10 C1 and C3. It could be indicated from the above phenomenon that insufficient odontoblast differentiation of the injected DMCs might occur at the lowest concentration of BMP4

used, thereby affecting the uniformity of the whole sample.

Masson and immunohistochemical staining (Fig. 11) further demonstrated the above condition. That is, regeneration of island-like tissues in all groups (25 μg/mL in Fig. 11 A and D; 12.5 μg/mL in Fig. 11 B and E; 6.25 μg/mL in Fig. 11 C and F) could be confirmed. Comparing the respective views of higher magnification (Fig. 11 A1-F1), the sample of 25 μg/mL had the best organized and mature dentinal tubules with strong staining for DSP (Fig. 11 A1 and D1). Polarized histological morphology of the regenerated tissues (Fig. 12 A-C) further confirmed the presence and organization of dentinal tubules of the three groups. Again, those well organized dentinal tubules could well be observed (Fig. 12 A), and such kind of structure became more and more compromised with the decrease in BMP4 concentration (Fig. 12 B).

A few reasons might account for why BMP-4 was chosen as a growth factor to initiate the above dentin-pulp regeneration process. First, it was reported that BMP-4 plays important roles in tooth development by participating in reciprocal epitheliomesenchymal induction and interaction.[58] It is also a crucial mesenchymal odontogenic signal which drives tooth morphogenesis through the bud-to-cap transition during tooth development.[59] Moreover, BMP-4 coordinated both the processes of dentin and enamel formation through both paracrine and autocrine ways in odontoblasts.[60,61] Due to its important roles mentioned in tooth morphogenesis, BMP-4 was taken as a morphogen to promote dentin-pulp complex regeneration in this work. As confirmed by current results, well vascularized dentin-pulp complex regeneration in nude mice model was achieved after the injection composed of HAG, DMCs and BMP-4 at an appropriate dosage. Second, it was shown in our previous study that when DMCs were combined with HAG scaffold and TGF-β1, dentin-pulp complex could be regenerated in nude mice, tooth slice models and even in situ in the empty pulp chamber of mini pigs.[1] In addition to identify that BMP-4 could also fulfill the similar task, the current work also confirmed the role of HAG. That is, HAG only acted as a delivery vehicle and also facilitated the non-specific morphogenesis as a three-dimensional hydrogel scaffold, and there was no special interaction between

HAG and TGF-β1. The role of HGA as a general scaffold could be thus indicated and its primary role appeared to be retention of cells, thereby facilitating the expected biological repair processes and morphogenesis.

Finally, it should be mentioned that the degradation of HAG could be tuned by the microenvironment, the presence of cells and cell physiological states. As to the implantation of pristine HAG, the duration was the longest among the three tried implantation conditions. It is possible that HAG could possibly have the flexibility to adjust its degradation under different environments. That is, cells or extracellular matrix within HAG scaffold could easily help to adjust its turnover, probably due to the biological nature of HA.

4. Conclusions

An HA based injectable scaffold has been successfully prepared by a crosslinking reaction of BDDE with HA to obtain HAG. The crosslinking degree could be adjusted simply by varying BDDE concentration. The higher the concentration of the crosslinker used, the more rigid the resulting hydrogel, subsequently the lower the swelling ratio would be and the higher the G' and G" values as well. Similar viscoelastic behaviors were found between HAGs and biological tissues, such as epidermis, dermis, articular cartilage and tooth germ, which accounts for the feasibility of using such HAG as an injectable scaffold for these tissue regeneration. HAG obtained at 0.4 vol% BDDE had pore diameters ranging from a few microns to around 100 μm with a high degree of interconnectivity, which was then demonstrated to be suitable for cartilage and pulp-dentin regeneration. The current study not only gave the detail on preparation, but could also be a reference to account how a crosslinked HA gel should be chosen for specific tissue regeneration.

Acknowledgement of financial support:

This study is financially supported by “the Fundamental Research Funds for the Central Universities”, National “973” Project Foundation (2010CB944804) and National Nature Science Foundation (81471855). The authors confirm that there are no known conflicts of interest associated with this publication.

References

1 L. Tan, J. Wang, S. Yin, W. Zhu, G. Zhou, Y. Cao and L. Cen, *RSC Adv.*, 2015, 5, 59723-59737.

2 M. Goldberg, and A. J. Smith, *Crit. Rev. Oral Biol. Med.*, 2004, 15, 13-27.

3 M. N. Collins and C. Birkinshaw, *Carbohydr. Polym.*, 2013, 92, 1262-1279.

4 I. L. Kim, R. L. Mauck and J. A. Burdick, *Biomaterials*, 2011, 32, 8771-8782.

5 M. S. Bae, J. Y. Ohe, J. B. Lee, D. N. Heo, W. Byun, H. Bae, Y. D. Kwon and I. K. Kwon, *Bone*, 2014, 59, 189-198.

6 W. Guo, Y. He, X. Zhang, W. Lu, C. Wang, H. Yu, Y. Liu, Y. Li, Y. Zhou, J. Zhou, M. Zhang, Z. Deng and Y. Jin, *Biomaterials,* 2009, 30, 6708-6723.

7 R. Li, W. Guo, B. Yang, L. Guo, L. Sheng, G. Chen, Y. Li, Q. Zou, D. Xie, X. An, Y. Chen, and W. Tian, *Biomaterials*, 2011, 32, 4525-38.

8 Y. Sapir, O. Kryukov and S. Cohen, *Biomaterials*, 2011, 32, 1838-1847.

9 J. Dahlmann, A. Krause, L. Moller, G. Kensah, M. Mowes, A. Diekmann, U. Martin, A. Kirschning, I. Gruh and G. Drager, *Biomaterials*, 2013, 34, 940-951.

10 R. Li, W. Guo, B. Yang, L. Guo, L. Sheng, G. Chen, Y. Li, Q. Zou, D. Xie, X. An, Y. Chen and W. Tian, *Biomaterials*, 2011, 32, 4525-4538.

11 K. Ren, C. He, C. Xiao, G. Li and X. Chen, *Biomaterials*, 2015, 51, 238-249.

12 A. Sivashanmugam, R. A. Kumar, M. V. Priya, S. V. Nair and R. Jayakumar, *J. Eur. Polym.*, 2015,72,543-565.

13 J. Radhakrishnan, U. M. Krishnan and S. Sethuraman, *Biotechnol. Adv.*, 2014, 32, 449-461.

14 Z. Liu and P. Yao, *Carbohydr. Polym.*, 2015, 132, 490-498.

15 M. Patenaude, N. M. Smeets and T. Hoare, *Macromol. Rapid Commun.*, 2014, 35, 598-617.

16 O. Qutachi, J. R. Vetsch, D. Gill, H. Cox, D. J. Scurr, S. Hofmann, R. Muller, R. A. Quirk, K. M. Shakesheff and C. V. Rahman, *Acta Biomater.*, 2014, 10, 5090-5098.

17 B. Balakrishnan, N. Joshi, A. Jayakrishnan and R. Banerjee, *Acta Biomater.*, 2014, 10, 3650-3663.

18 R. S. Moglia, J. L. Robinson, A. D. Muschenborn, T. J. Touchet, D. J. Maitland and E. Cosgriff-Hernandez, *Polymer*, 2014, 56, 426-434.

19 J. D. Kretlow, L. Klouda and A. G. Mikos, *Adv. Drug Deliv. Rev.*, 2007, 59, 263-273.

20 A. Gutowska, B. Jeong and M. Jasionowski, *Anat. Rec.*, 2001, 263, 342-349.

21 J. B. Luan, W. J. Shen, C. Chen, K.W. Lei, L. Yu and J. D. Ding, *RSC Adv.*, 2015, 5, 97975-97981.

22 L. P. Cao, B. Cao, C. J. Lu, G. W. Wang, L. Yu and J. D. Ding, *J Mater. Chem. B*, 2015, 3, 1268-1280.

23 W. J. Shen, J. B. Luan, L. P. Cao, J. Sun, L. Yu and J. D. Ding, *Biomacromolecules*, 2015, 16, 105-115.

24 K. W. Lei, W. J. Shen, L. P. Cao, L. Yu and J. D. Ding. *Chem. Commun.*, 2015, 51, 6080-6083.

25 L. Yu, H. Zhang and J. D. Ding. *Angew. Chem. Int. Ed.*, 2006, 45, 2232-2235.

26 J. Necas, L. Bartosikova, P. Brauner, and J. Kolar, *Vet. Med.*, 2008, 53, 397-411.

27 N. Cui, J. Qian, T. Liu, N. Zhao and H. Wang, *Carbohydr. Polym.*, 2015, 126, 192-198.

28 J. Y. Kang, C. W. Chung, J. H. Sung, B. S. Park, J. Y. Choi, S. J. Lee, B. C. Choi, C. K. Shim, S. J. Chung and D. D. Kim, *Int. J. Pharm.*, 2009, 369, 114-120.

29 C. Yang, X. Wang, X. Yao, Y. Zhang, W. Wu and X. Jiang, *J. Control. Release*, 2015, 205, 206-217.

30 H. S. Yoo, E. A. Lee, J. J. Yoon and T. G. Park, *Biomaterials*, 2005, 26, 1925-1933.

31 W. H. Chen, W. C. Lo, W. C. Hsu, H. J. Wei, H. Y. Liu, C. H. Lee, S. Y. Tina Chen, Y. H. Shieh, D. F. Williams and W. P. Deng, *Biomaterials*, 2014, 35, 9599-9607.

32 S. Felszeghy, M. Hyttinen, R. Tammi, M. Tammi, and L. Módis, *Eur. J. Oral Sci.*, 2000, 108, 320-326.

33 T. Sasaki, H. And Kawamata-Kido, *Arch. Oral Biol.*, 1995, 40, 209-219.

34 X. Xu, A. K. Jha, D. A. Harrington, M. C. Farach-Carson and X. Jia, *Soft Matter*, 2012, 8, 3280-3294.

35 K. D. Boulle, R. Glogau, T. Kono, M. Nathan, A. Tezel, J. X. Roca-Martinez, S. Paliwal and D. Stroumpoulis, *Dermatol. Surg.*, 2013, 39, 1758-1766.

36 H. Feng, G. Zhang, Y. Xu, Y. Ni, and W. Sun, Chin. J. *Pharm. Anal.*, 2012, 32, 654-657.

37 X. Liu, G. Zhou, W. Liu, W. Zhang, L. Cui and Y. Cao, *Biotechnol. Lett.*, 2007, 29, 1685-1690.

38 J. Liu, X. Liu, G. Zhou, R. Xiao and Y. Cao, *Anat. Rec.*, 2012, 295, 1109-1116.

39 J. Xue, B. Feng, R. Zheng, Y. Lu, G. Zhou, W. Liu, Y. Cao, Y. Zhang and W. Zhang, *Biomaterials*, 2013, 34, 2624-2631.

40 B. R. Snyder, P. H. Cheng, J. Yang, S. H. Yang, A. H. Huang and A. W. Chan, *BMC Cell Biol.*, 2011, 12, 39-46.

41 S. S. Prime and B. H. Toh, *J. Cell Sci.*, 1978, 33, 329-340.

42 D. E. Discher, P. Janmey and Y. Wang, *Science*, 2005, 310, 1139-1143.

43 R. J. Jr. Pelham and Y. Wang, *Proc. Natl. Acad. Sci. USA*, 1997, 94, 13661-13665.

44 E. S. Place, N. D. Evans, and M. M. Stevens, *Nat. Mater.*, 2009, 8, 457-470.

45 F. S. Brandt, and A. Cazzaniga, *Clin. Interv. Aging*, 2008, 3, 153-159.

46 M. H. Gold, Clin. Interv. *Aging*, 2007, 2, 369-376.

47 D. W. Buck, 2nd, M. Alam, and J. Y. Kim, *J. Plast. Reconstr. Aesthet. Surg.*, 2009, 62, 11-18.

48 G. D. Monheit, and C. L. Prather, *Dermatol. Ther.*, 2007, 20, 394-406.

49 J. Kablik, G. D. Monheit, L. Yu, G. Chang and J. Gershkovich, *Dermatol. Surg.*, 2009, 35, 302-312.

50 A. Tezel, and G. H. Fredrickson, *J. Cosmet. Laser. Ther.*, 2008, 10, 35-42.

51 Y. Liu , X. Z. Shu, and G. D. Prestwich, *Tissue Eng.*, 2006, 12, 3405-3416.

52 J. Elisseeff, *Expert Opin. Biol. Ther.*, 2004, 4, 1849-1859.

53 J. Elisseeff, K. Anseth, D. Sims, W. Mcintosh, M. Randolph, and R. Langer, *Proc. Natl. Acad. Sci. USA*, 1999, 96, 3104-3107.

54 K. S. Anseth, A. T. Metters, S. J. Bryant, P. J. Martens, J. H. Elisseeff, and C. N. Bowman, *J. Control. Release*, 2002, 78, 199-209.

55 J. A. Burdick, and G. D. Prestwich, *Adv. Mater.*, 2011, 23, H41-56.

56 M. S. Kim, S. J. Park, B. K. Gu, and C. H. Kim, *Carbohydr. Polym.*, 2012, 87, 2683-2689.

57 H. Shen, Y. Niu, X. Hu, F. Yang, S. G. Wang, and D. C. Wu, *J. Mater. Chem. B*, 2015, 3, 4417-4425.

58 S. Jia , J. Zhou , Y. Gao , J. A. Baek, J. F. Martin, Y. Lan and R. J, *Development*, 2013, 140, 423-432.

59 T. Aberg, J. Wozney, and I. Thesleff, *Dev. Dyn.*, 1997, 210, 383-396.

60 J. Gluhak-Heinrich, D. Guo, W. Yang, M. A. Harris, A. Lichtler, B. Kream, J. Zhang, J. Q. Feng, L. C. Smith, P. Dechow and S. E. Harris, *Bone*, 2010, 46, 1533-1545.

61 Y. Li, X. Lü, X. Sun, S. Bai, S. Li, and J. Shi, *Arch. Oral Biol.*, 2011, 56, 1221-1229.

Figure Captions:

Figure 1. Swelling ratio of HA hydrogels crosslinked with different concentrations of BDDE. BDDE concentrations used to crosslink HA were 0.4 vol%, 0.6 vol%, 0.8 vol% and1.0 vol%, respectively.

Figure 2. Dynamic oscillatory frequency sweep curves for HA hydrogels crosslinked with different concentrations of BDDE. Storage modulus (a) and loss modulus (b) at 37 ^{o}C as a function of frequency (Hz) for HA hydrogels crosslinked with different concentrations of BDDE (0.4 vol%, 0.6 vol%, 0.8 vol%, 1.0 vol%).

Figure 3. Dynamic oscillatory frequency sweep curves for porcine epidermis, dermis, cartilage and tooth germ. Storage modulus (a) and loss modulus (b) at 37 ^{o}C as a function of frequency (Hz) for epidermis, dermis, cartilage and tooth germ, respectively.

Figure 4. Scanning electron microscopic images of the cross-section of HA hydrogels crosslinked with different concentrations of BDDE. BDDE concentrations used to crosslink HA were 0.4 vol% (A1, A2), 0.6 vol% (B1, B2), 0.8 vol% (C1, C2) and 1.0 vol% (D1, D2), respectively.

Figure 5. Microscopic images of HA injectable gel particles. HA injectable gel particles were prepared by being crosslinked with 0.4 vol% BDDE. (B) is a higher magnification view of (A).

Figure 6. In vitro cytotoxicity assay of HA gel on human fibroblasts. Human fibroblasts in their logarithmic growth were seeded at a density of 5×10^3 cells per well in 96-well plates with 100 μL of culture medium, respectively. After 24 h of incubation, the medium was replaced with 100 μL of the above culture medium (negative control), or 100 μL medium containing either 0.5 mg/mL or 1 mg/mL HA gels, or 100 μL medium containing 64 mg/mL phenol (positive control), respectively. Cells were incubated with these treatments for 2 d, 4 d or 7 d, respectively, and the respective viability of cells was then determined by MTT assay. HA gel was cross-linked by 0.4 vol% BDDE concentration. Values are the absorbance of each well at a wavelength of 490 nm, expressed as mean ± sd of three experiments, assayed in quintuple. The level of significance was set at $P < 0.05$. *$P < 0.05$ vs. negative control, $^{\diamond}P < 0.05$ vs. positive control, $^{\#}P < 0.05$ vs. 0.5 mg/mL.

Figure 7. Gross view and histological analysis of HAG scaffolds injected subcutaneously in nude mice for 15 and 36 weeks. A and B were gross views of the samples injected for 15 and 36 weeks, respectively. A1 and B1 were overall views of H&E staining of the samples injected for 15 and 36 weeks, respectively. A2 and A3, B2 and B3 were higher magnification observations of the localized square areas within A and B, respectively. No specific tissue was regenerated in HAG scaffold injected either for 15 (A2-A3) or 36 (B2-B3) weeks. A few fibroblasts encapsulating

the HAG scaffolds could be observed at both time points (A3, B3). HAG fragments were labeled by green arrow heads. Scale bars: 1000 μm for A1 and B1; 50 μm for A2-A3 and B2-B3.

Figure 8. Regeneration of cartilage-like tissue using HAG. (A) In vivo construction process after being injected subcutaneously in nude mice. The inset in (A) was the gross view of the tissue harvested after being constructed subcutaneously in nude mice for 12 weeks. The tissues were constructed using chondrocytes (2×10^7 cells/mL) and HAG. (B) Overall view of H&E staining of the regenerated tissue. (C) was the localized square area of higher magnification observation within (B). Scale bars: 1000 μm for B; 100 μm for C.

Figure 9. Regeneration of dentin-pulp like tissue using HAG. In vivo construction process immediately after injection (A) and before sample harvest (B). Gross views of regenerated tissues constructed subcutaneously in nude mice for 10 weeks using DMCs (5×10^7 cells/mL), HAG, and BMP-4 of 25 μg/mL (C), 12.5 μg/mL (D), and 6.25 μg/mL (E), respectively.

Figure 10. Histological analysis of the regenerated tissue constructed subcutaneously in nude mice for 10 weeks. The tissues were constructed using DMCs (5×10^7 cells/mL), HAG, and BMP-4 of different concentrations (25 μg/mL in A, A1-A3; 12.5 μg/mL in B, B1-B3; 6.25 μg/mL in C, C1-C3). Overall views of H&E (A, B and C) staining of the respective regenerated tissues. All tissues in A, B and C exhibited typical island-like features. A1, A2, B1, and C1 were higher magnification observations of the localized square areas within A, B, and C, respectively. A3, B2, B3, C2, and C3 were higher magnification observations of the localized square areas within A1, B1, and C1 respectively. There were well-organized dentinal-like tubules (white arrow head) arranged radially along the pulp-like tissue and columnar odontoblast-like cells with polarized basal nuclei (yellow arrow head) lining up along the dentinal wall (A1-A3). Although dentinal-like tubules (white arrow head) and columnar odontoblast-like cells (yellow arrow head) could also be observed within B1-B3 and C2, such structure was not well organized as that in A1-A3. Moreover, bone-like tissue formation in C1 and C3 was observed even with hypertrophic cells (C3), indicating that insufficient differentiation occurred in the current sample. Blood vessels were distributed within all of these tissues (black arrow head). Scale bars: 1000 μm for A, B and C; 100 μm for A1, B1 and C1; 50 μm for A2-A3, B2-B3 and C2-C3.

Figure 11. Masson and immunohistochemical staining of the regenerated tissues constructed subcutaneously in nude mice for 10 weeks. The tissues were constructed using DMCs (5×10^7 cells/mL), HAG, and BMP-4 of different concentrations (25 μg/mL in A and D; 12.5 μg/mL in B and E; 6.25 μg/mL in C and F). A, B and C were overall views of Masson staining of the different tissues. A1, B1, and C1 are higher magnification observations of the localized square areas within A, B, and C, respectively. D, E, and F were overall views of immunohistochemical staining for

dentin sialoprotein (DSP) of the different tissues. D1, E1, and F1 were higher magnification observations of the localized square areas within D, E, and F respectively. DSP positive staining could be observed throughout the whole structures of D, E, and F, especially within areas of soft tissues. Strong DSP staining of those dentinal tubules could only be observed in D1. The positive DSP expression by odontoblast-like cells were indicated by yellow arrow heads, while DSP staining by dentinal tubules were indicated by white arrow heads. Scale bars: 1000 μm for A, B, C, D, E and F; 50 μm for A1, B1, C1, D1, E1 and F1.

Figure 12. Polarized histological morphology of the regenerated tissues constructed subcutaneously in nude mice for 10 weeks. The tissues were constructed using DMCs (5×10^7 cells/mL), HAG, and BMP-4 of different concentrations (25 μg/mL in A-A2; 12.5 μg/mL in B-B2; 6.25 μg/mL in C-C2). A1, B1, and C1 were higher magnification polarized H&E observations of A, B, and C, respectively, while A2, B2, and C2 were higher magnification polarized H&E observations of A1, B1, and C1, respectively,. Scale bars: 200 μm for A, B and C; 100 μm for A1, B1 and C1; 50 μm for A2, B2 and C2.

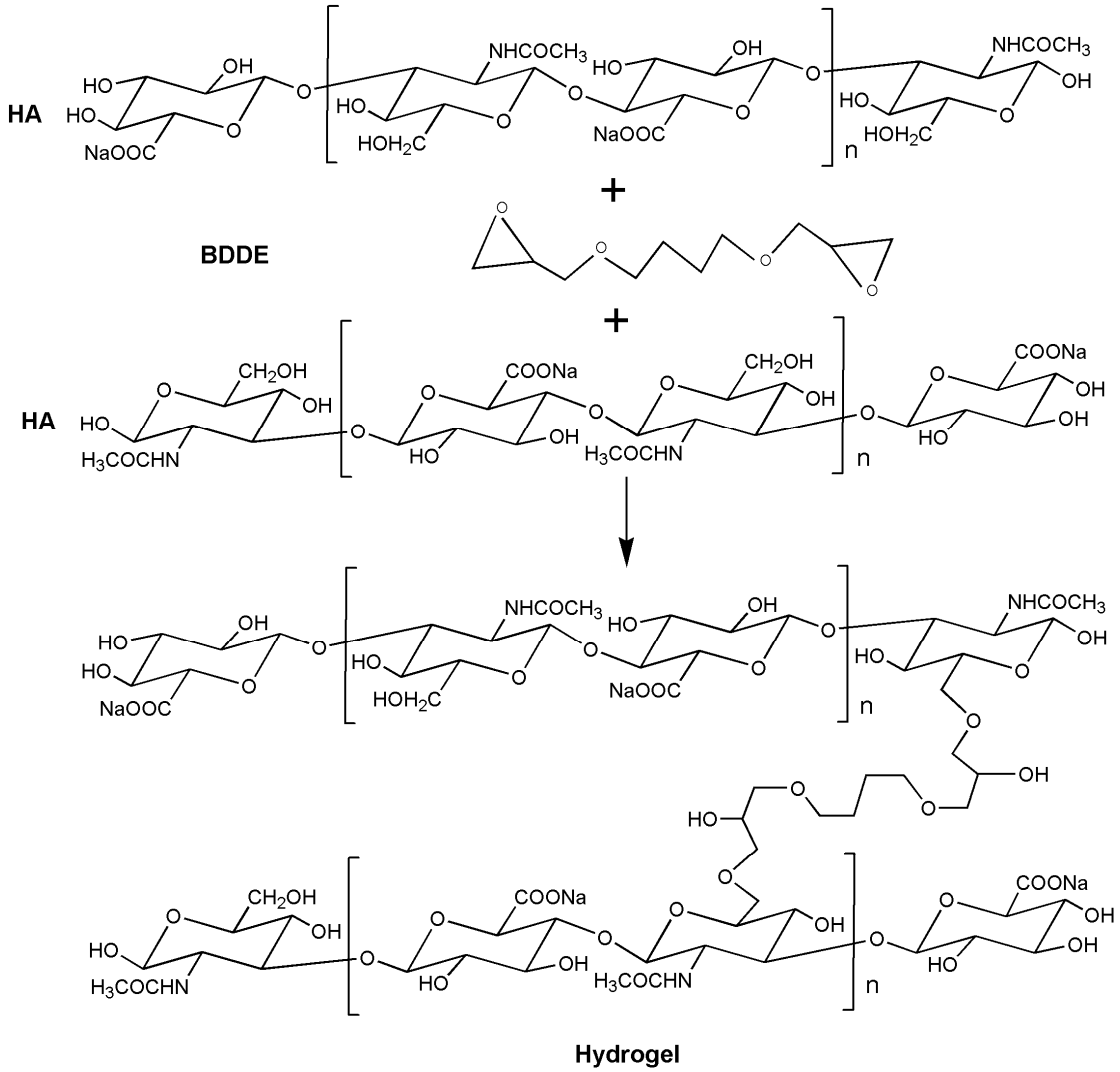

Scheme 1. Illustration of the crosslinking reaction of HA with 1,4-butanediol diglycidyl ether BDDE. HA: hyaluronic acid; BDDE: 1,4-butanediol diglycidyl ether.

Table 1. Release of BDDE residue by crosslinked HA hydrogels

BDDE concentration (%)	First release (μg)	Second release (μg)	Third release (μg)	Fourth release (μg)	Total release (μg)
0.4	158.5	83	15	/	256.5
0.6	226	106.5	41.5	11	385
0.8	294	147.5	57.5	16.5	515.5
1.0	366	162	93.5	26.5	648

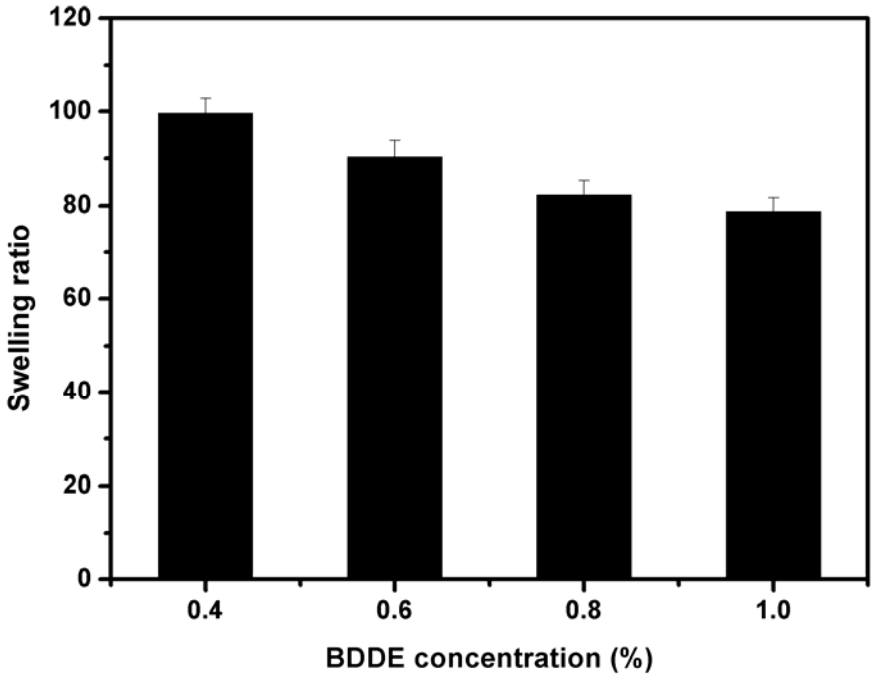
120
100
80
60
40
20
0
Swelling ratio
0.4
0.6
0.8
1.0
BDDE concentration (%)

Figure 1.

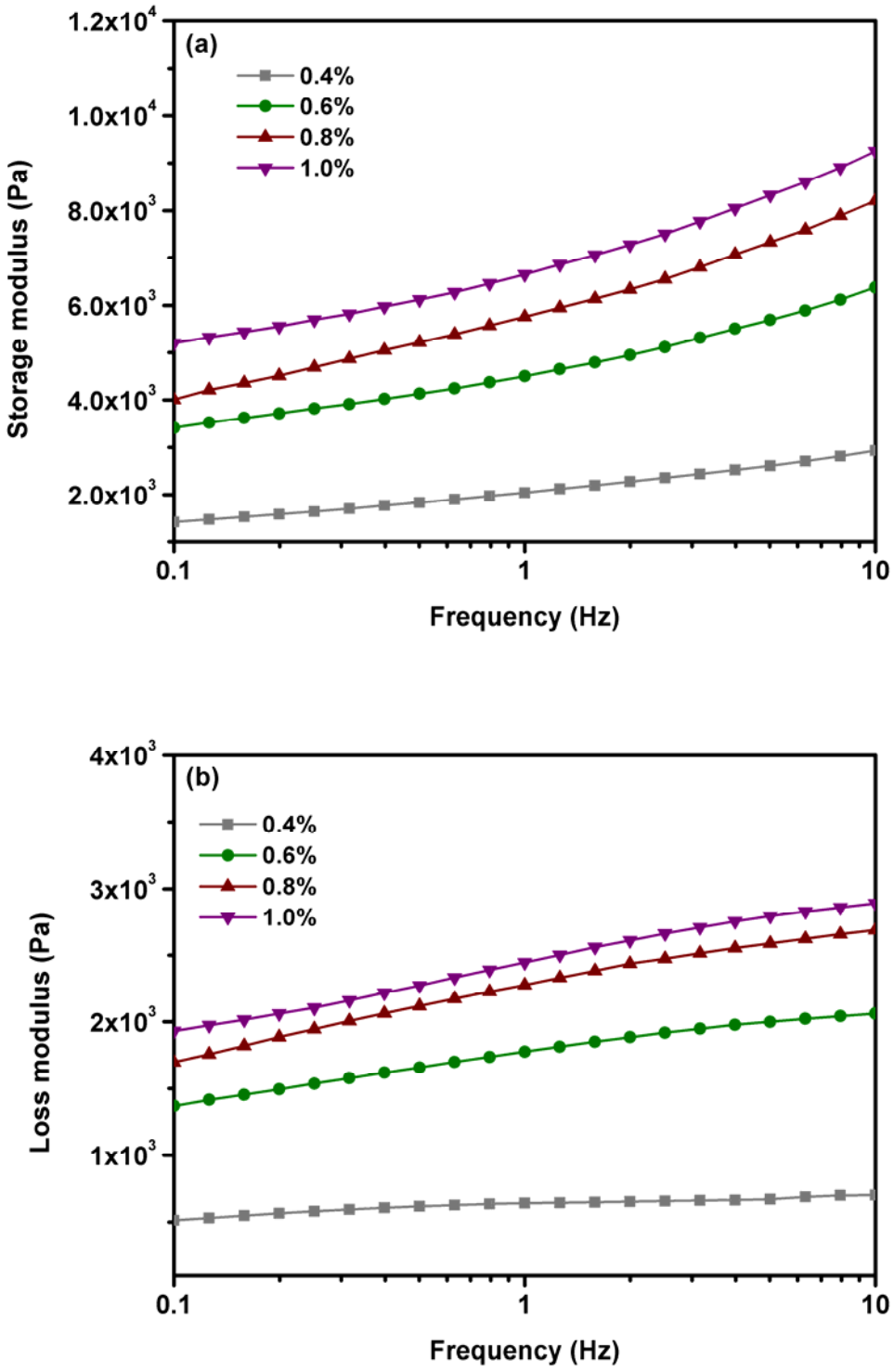
(a)
0.4%
0.6%
0.8%
1.0%
Storage modulus (Pa)
1.2x10^4
1.0x10^4
8.0x10^3
6.0x10^3
4.0x10^3
2.0x10^3
0.1
1
10
Frequency (Hz)
(b)
0.4%
0.6%
0.8%
1.0%
Loss modulus (Pa)
4x10^3
3x10^3
2x10^3
1x10^3
0.1
1
10
Frequency (Hz)

Figure 2.

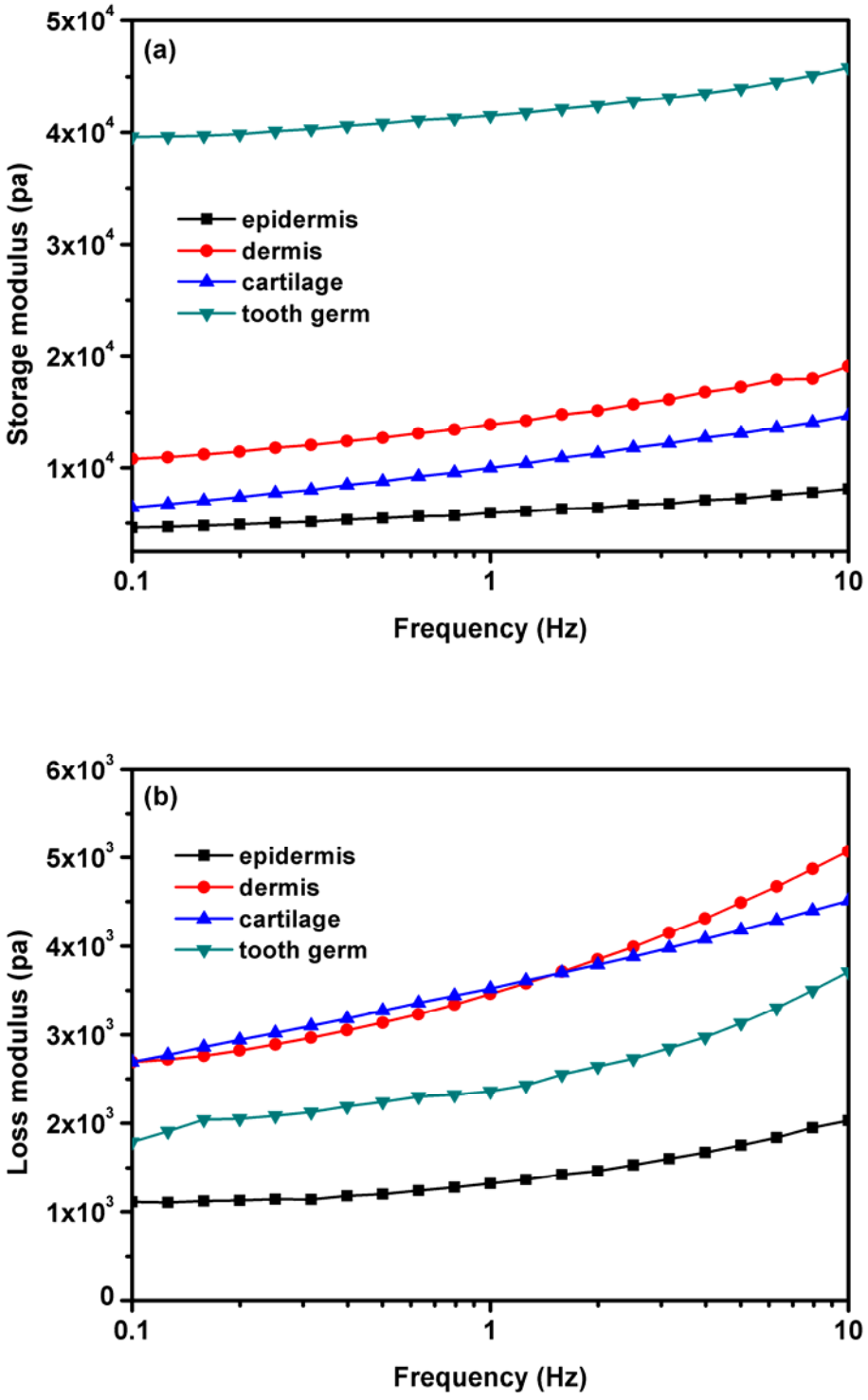
(a)
Storage modulus (pa)
5x10^4
4x10^4
3x10^4
2x10^4
1x10^4
epidermis
dermis
cartilage
tooth germ
0.1
1
10
Frequency (Hz)
(b)
Loss modulus (pa)
6x10^3
5x10^3
4x10^3
3x10^3
2x10^3
1x10^3
0
epidermis
dermis
cartilage
tooth germ
0.1
1
10
Frequency (Hz)

Figure 3.

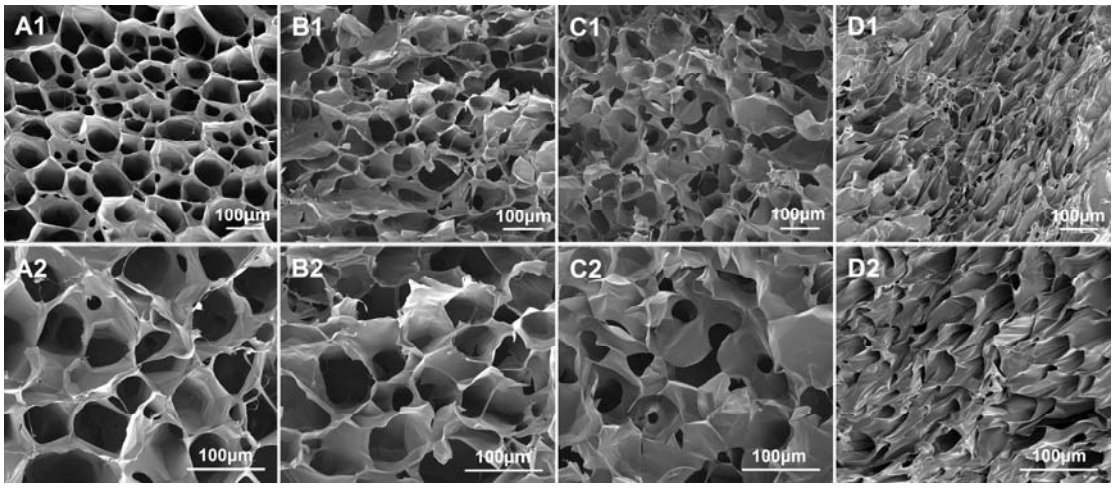
A1
B1
C1
D1
100μm
100μm
100μm
100μm
A2
B2
C2
D2
100μm
100μm
100μm
100μm

Figure 4.

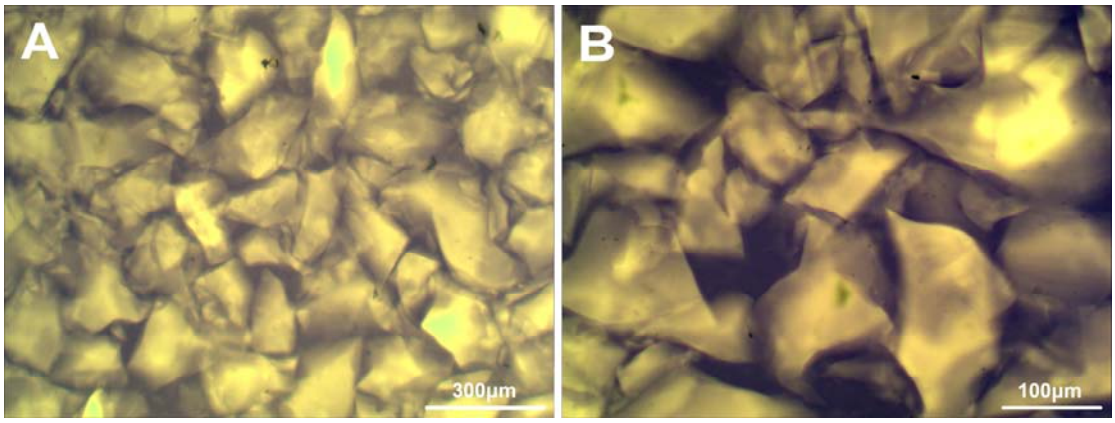

Figure 5.

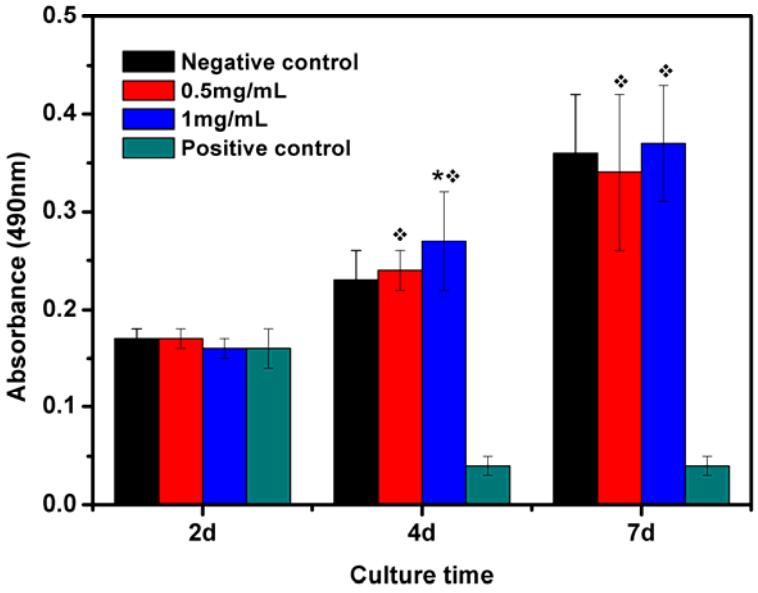
Negative control
0.5mg/mL
1mg/mL
Positive control
Absorbance (490nm)
0.0
0.1
0.2
0.3
0.4
0.5
2d
4d
7d
Culture time
*❖
❖
❖
❖

Figure 6.

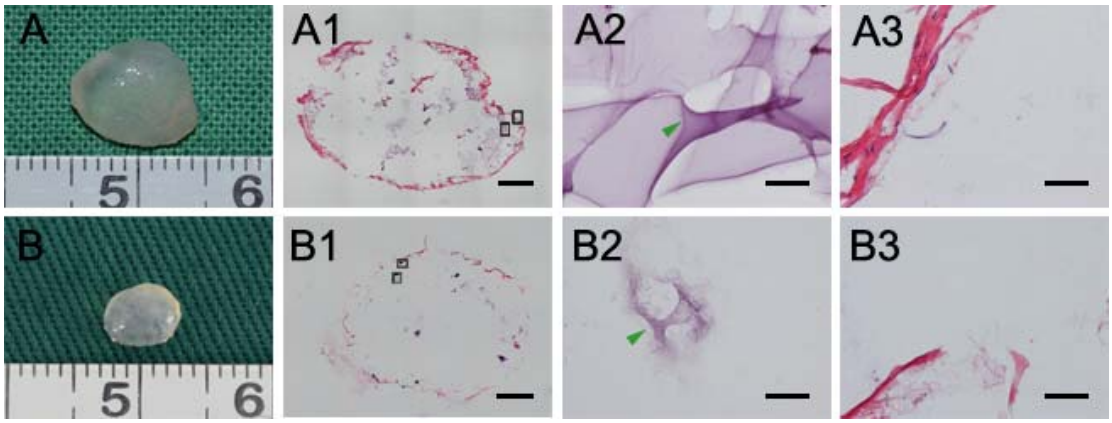

Figure 7.

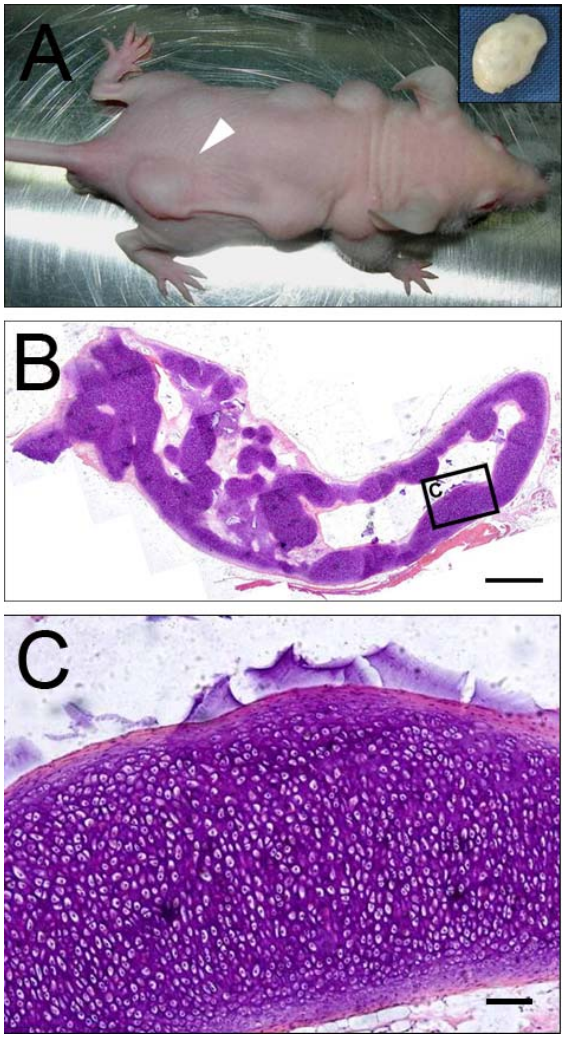

Figure 8.

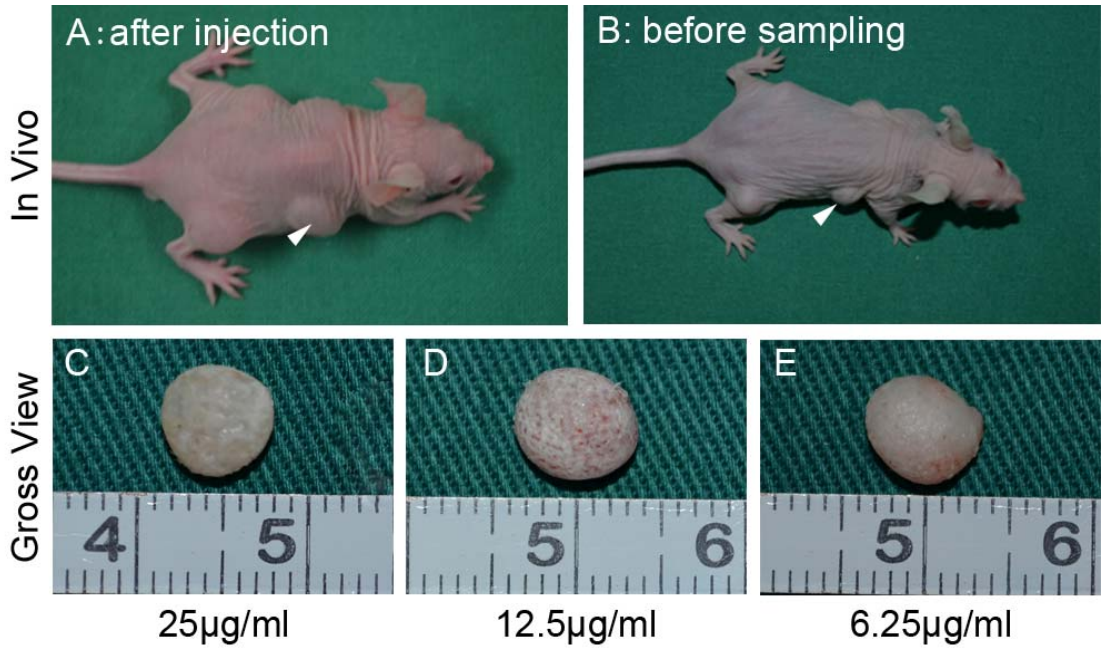
A : after injection
B: before sampling
In Vivo
Gross View
C
D
E
25μg/ml
12.5μg/ml
6.25μg/ml

Figure 9.

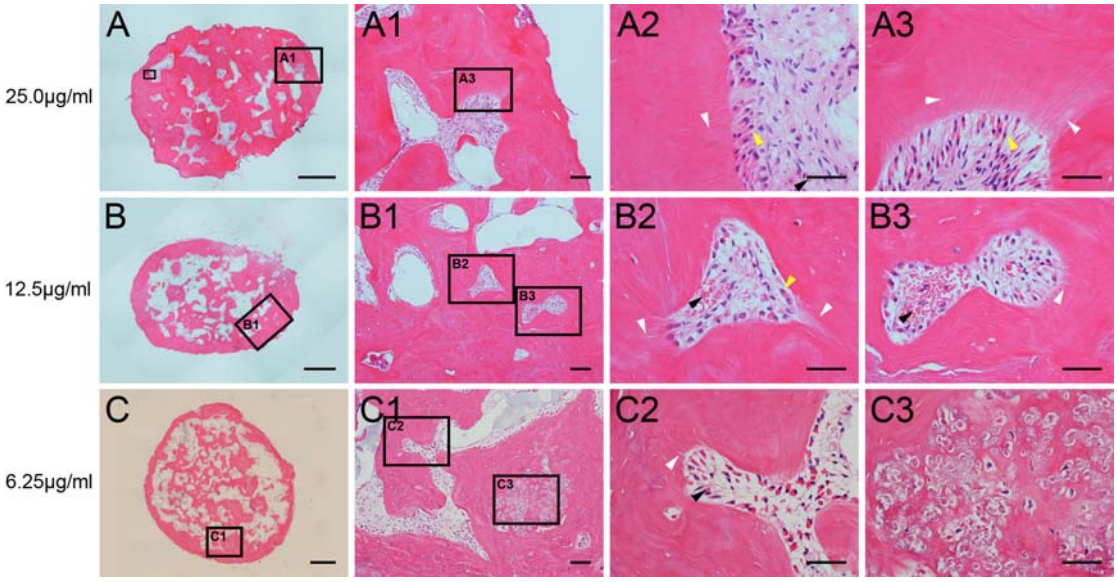

Figure 10.

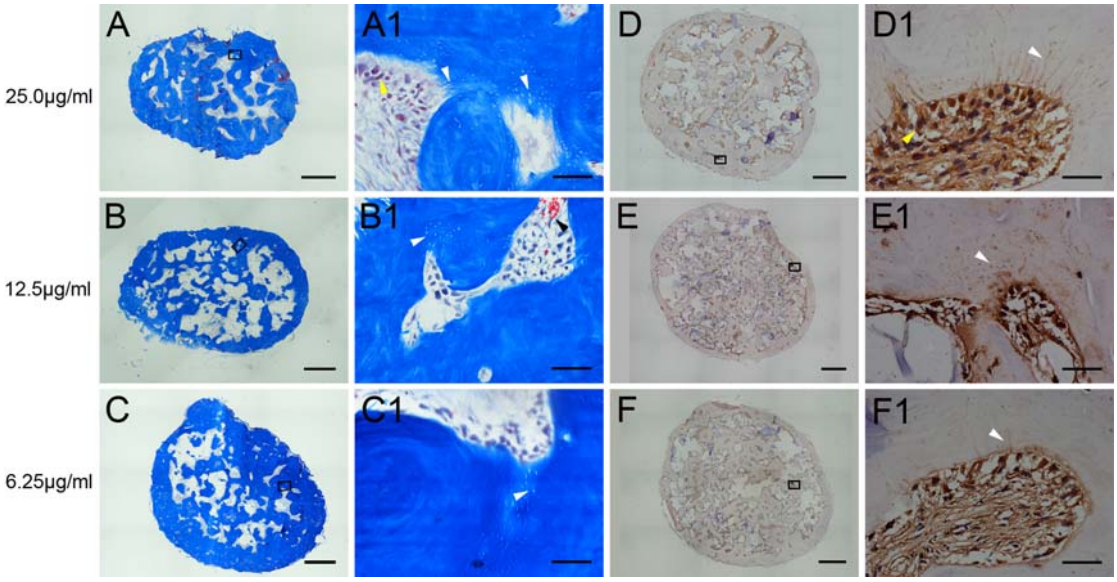

Figure 11.

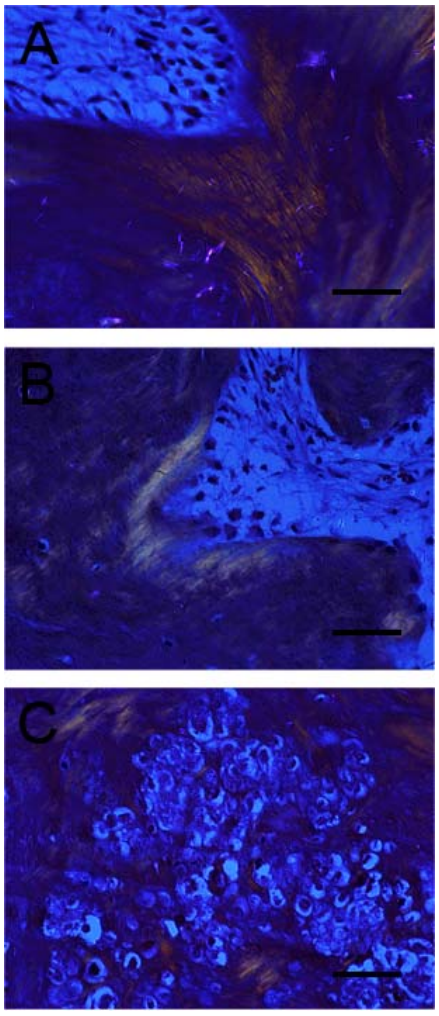

Figure 12.

TOC

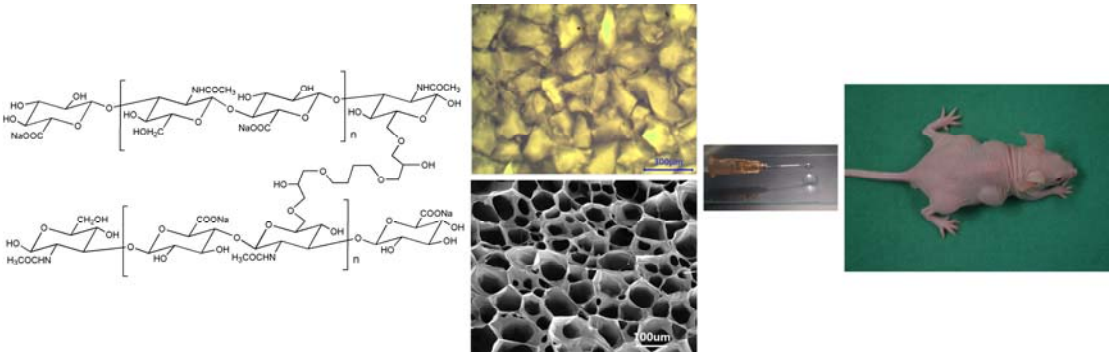

An injectable scaffold of crosslinked hyaluronic acid gel for tissue regeneration